Uracil-DNA glycosylase is not implicated in the choice of the DNA repair pathway during B-cell class switch recombination.

Nour Ghazzaui[1,2], Hussein Issaoui[1,2], Alexis Saintamand[3], Yves Denizot[1,4], François Boyer[1]

[1]UMR CNRS 7276, INSERM U1262, University of Limoges, CBRS, rue Pr. Descottes, 87025 Limoges, France

[2]N.G. and H.I. contributed equally to this work.

[3]present address: INSERM U1236, Rennes 1 University, France

[4]To whom correspondence should be addressed. Email: yves.denizot@unilim.fr

Running title: UNG and B-cell class switch recombination.

Acknowledgments: We thank Dr. Tomas Lindahl for sending us UNG-deficient mice. This work was supported by ANR (projet EpiSwitch-3'RR 2016). N.G. was supported by a grant from Association de Spécialisation et d'Orientation Scientifique (Lebanon) and the municipality of Khiam (Lebanon). H.I. is supported by CORC (FJA/NP 2015-109) and University of Limoges. The authors are "Equipe Labellisée LIGUE 2018". We thank the GénoLim platform and the Cytometry platform of the University of Limoges for sequencing and cell sorting. F.B. is supported by Fondation Partenariale de l'Université de Limoges and ALURAD.

The authors declare no conflict of interest.

Author contributions: Y.D designed research. N.G., H.I. and A.S. performed research. A.S., F.B and Y.D. analysed data. A.S, F.B and Y.D. wrote the paper.

Mature B-cells express membrane IgM and IgD (of same specificity) through alternative splicing of a pre-mRNA encompassing constant ($C)_\mu$ and C_δ genes. After encountering antigen, B-cells undergo class switch recombination (CSR) that substitutes the C_μ gene with C_γ, C_ε or C_α, thereby generating IgG, IgE and IgA antibodies with same antigenic specificity but new effector functions. The DNA-editing enzyme activation-induced deaminase (AID) is essential to CSR by targeting switch (S) regions preceding C_μ (namely the S_μ donor region) and C_γ, C_ε and C_α genes (namely the $S_{\gamma,\varepsilon,\alpha}$ acceptor regions) (1, 2). CSR is controlled in *cis* by IgH locus super-enhancers (3) and in *trans* by a wide spectrum of enzymes and proteins (1, 2). Among them the role of the uracil DNA glycosylase (UNG) remains controversial. UNG is a key enzyme of the base excision repair (BER) component that carries out faithful repair. Some authors estimate that during CSR the UNG enzymatic activity removes the AID-induced dC to dU converted base of single strand DNA generating abasic sites thus leading to DNA strand breaks (1). For other authors the role of UNG is to stabilize the S-S synapse and to recruit DNA repair factors that facilitate the end-joining process (4, 5). Thus, the classical non-homogenous end joining (c-NHEJ) pathway would be increased over the alternative end joining (A-EJ) in UNG deficient mice (4) suggesting an intriguing role of UNG in favour of the A-EJ way. These results were based on the analysis of few S_μ-$S_{\gamma1}$ sequences obtained in UNG deficient conditions due to technical limitations (conventional Sanger sequencing) to investigate S-S junction molecular signatures. We recently reported a new computational tool (CSReport) for automatic analysis of CSR junctions sequenced by high-throughput sequencing (6). We have used it to analyze the rare S_μ-σ_δ junctions form during IgD CSR (7, 8) and S_μ-$S_{\gamma3,}$ S_μ-$S_{\gamma1}$ and S_μ-S_α junctions in *wt* mice (9). We thus used CSReport and high-throughput sequencing to analyze the molecular signature of S_μ-$S_{\gamma3,}$ S_μ-$S_{\gamma1}$ and S_μ-S_α junctions in UNG deficient mice more in depth.

Our research has been approved by our local ethics committee review board (Comité Régional d'Ethique sur l'Expérimentation Animale du Limousin, Limoges, France) and carried according the European guidelines for animal experimentation. Wild-type (*wt*) mice and UNG-deficient mice (a gift from Dr. Tomas Lindahl, UK) were used. Single-cell suspensions of spleen cells were cultured

4 days at $1x10^6$ cells/ml in RPMI 1640 with 10% fetal calf serum and 5 μg/ml LPS, with (CSR toward IgG_1) or without (CSR toward IgG_3) addition of 20 ng/ml IL-4 or 2 ng/ml TGFβ (PeproTech, Rocky Hill, NJ) (CSR toward IgA) (3, 9, 10). Splenocytes were washed in PBS and stained with various antibodies: anti-B220-PC5, anti-CD138-APC, anti-IgM PECy7, anti-IgG_3-FITC, anti-IgG_1-FITC and anti-IgA-FITC. Cells were analyzed on a Fortessa LSR2 (Beckman Coulter). In paralleled experiments, stimulated splenocyte DNA was extracted for investigation of S_μ-$S_{\gamma 3}$, S_μ-$S_{\gamma 1}$ and S_μ-S_α junctions. As previously described in detail (6), junctions were PCR amplified. Libraries of 200bp were prepared from the 1-2kb PCR products of S_μ-$S_{\gamma 1}$, S_μ-$S_{\gamma 3}$ and S_μ-S_α amplification for Ion Proton sequencing ("GénoLim platform" of the Limoges University, France). Sequenced reads were then mapped to S_μ, $S_{\gamma 1}$, $S_{\gamma 3}$ and S_α regions using BLAST algorithm. The computational tool developed for experiments performs junction assembly, identifies breakpoints in S_μ, $S_{\gamma 1}$, $S_{\gamma 3}$ and S_α, identifies junction structure (blunt, micro-homology, large-homology or junction with insertions) and outputs a statistical summarization of identified junctions.

The UNG deficiency markedly reduces CSR toward IgG_3 (mean 0.1% *vs* 6.9%), IgG_1 (mean 1.9% *vs* 14.7%) and IgA (mean 1.4% *vs* 2.5%) compared to *wt* mice (Fig. 1A). After DNA extraction the molecular signatures of S_μ-$S_{\gamma 1}$, S_μ-$S_{\gamma 3}$ and S_μ-S_α junctions were investigated. The structural profiles of S_μ-$S_{\gamma 1}$, S_μ-$S_{\gamma 3}$ and S_μ-S_α junctions (blunt, micro-homology, large-homology or junction with insertions) for UNG-deficient and *wt* mice are reported in Fig. 1B. The distributions of IgG_1, IgG_3 and IgA junctions in terms of distance from the forward PCR primer in S_μ and from of one of the reverse primers in $S_{\gamma 3}$, $S_{\gamma 1}$ and S_α are reported in Fig. 1C. Localizations of breakpoints within AID hotspots (AGCT, WRCY, RGYW) and other motifs are shown in Fig. 1D (displayed along specifically targeted segments within S regions).

Data indicated that if UNG deficiency markedly affected CSR efficiency, it did not significantly affect the pattern of blunt *vs* micro/large-homology remaining junctions. Similarly the positions of IgG_3, IgG_1 and IgA junctions (in term of distance from S_μ and $S_{\gamma 1,\gamma 3,\alpha}$) and their colocation with

AID-attack motifs were not affected. Summarization of these 1568 independent junctions provided description of CSR sequences in UNG-deficient mice at an unprecedented level. Until now only few had been reported after cloning and subsequent sequencing by Sanger's method (4). In this latter study, the panel of *wt* junctions was markedly different (in terms of blunt *vs* micro-homology junctions) from ours and those of Panchakshari and coll. (2). Our results undoubtedly demonstrate that CSR in UNG deficient conditions did not affect the balance between N-HEJ and A-EJ. These results also show that μ-γ_1, μ-γ_3 and μ-α CSR in UNG-deficient mice are regulated and that double strand breaks for IgG1, IgG3 and IgA CSR are not random breaks. In conclusion our results strengthen the hypothesis that during AID induced CSR, UNG in association with recombination factors may facilitate the stabilization of the S-S synapse to facilitate an efficient recombination. In contrast our results do not argue in favor of an UNG role in the recruitment of specific DNA repair factors.

References

1. Chaudhuri J, Alt FW. Class-switch recombination: interplay of transcription, DNA deamination and DNA repair. Nat Rev Immunol 2004; 4: 541-552.

2. Panchakshari RA, Zhang X, Kumar V, Du Z, Wei PC, Kao J et al. DNA double-strand break response factors influence end-joining features of IgH class switch and general translocation junctions. Proc Natl Acad Sci USA 2018; 115: 762-767.

3. Saintamand A, Rouaud P, Saad F, Rios G, Cogné M, Denizot Y. Elucidation of IgH 3' region regulatory role during class switch recombination via germline deletion. Nature Commun 2015; 6: 7084.

4. Yousif AS, Stanlie A, Mondal S, Honjo T, Begum NA. Differential regulation of S-region hypermutation and class-switch recombination by noncanonical functions of uracil DNA glycosylase. Proc Natl Acad Sci USA 2014; 111: E1016-E1024.

5. Yousif AS, Stanlie A, Begum NA, Honjo T. Opinion: uracil DNA glycosylase (UNG) plays distinct and non-canonical roles in somatic hypermutation and class switch recombination. Int Immunol 2014; 26: 575-578.

6. Boyer F, Boutouil H, Dalloul I, Dalloul Z, Cook-Moreau J, Aldigier JC et al. CSReport: a new computational tool designed for automatic analysis of class switch recombination junctions sequenced by high-throughput sequencing. J Immunol 2017; 198: 4148-4155.

7. Ghazzaui N, Issaoui H, Saintamand A, Boyer F, Denizot Y. Analysis of IgD CSR junctions by high-throughput sequencing. Immunol Lett 2017; 188: 86-88.

8. Issaoui H, Ghazzaui N, Saintamand A, Denizot Y, Boyer F. IgD class switch recombination is not controlled through the immunoglobulin heavy chain 3' regulatory region super-enhancer. Cell Mol Immunol 2017; 14: 871–874.

9. Issaoui H, Ghazzaui N, Saintamand A, Denizot Y, Boyer F. High throughput sequencing reveals similar molecular signatures for class switch recombination junctions for the γ and α isotypes. Cell Mol Immunol 2018 Mar 23. doi: 10.1038/s41423-018-0025-z. [Epub ahead of print]

10. Issaoui H, Ghazzaui N, Saintamand A, Carrion C, Oblet C, Denizot Y. The IgH 3' regulatory region super-enhancer does not control IgA class switch recombination in the B1 lineage. Cell Mol Immunol 2018; 15: 289-291.

Legends to Figure

Figure 1: Class switch recombination in UNG-deficient and *wt* mice.

A: IgG_1, IgG_3 and IgA CSR in UNG-deficient and *wt* mice. Spleen cells were LPS-cultured 4 days with (CSR toward IgG_1) or without (CSR toward IgG_3) addition of IL-4 or TGFβ (CSR toward IgA). Cells gated on $B220^+$ and/or $CD138^+$ cells were investigated with anti-IgMPECy5, anti-IgG_3-FITC, anti-IgG_1-FITC and anti-IgA-FITC antibodies. One representative experiment out of three to five for each genotype is shown. B: Structure profiles of S_μ-$S_{\gamma 1}$, S_μ-$S_{\gamma 3}$ and S_μ-S_α junctions in UNG-

deficient and wt mice. Junctions are classified in terms of junction types (junction with insertions, blunt junction, junction with micro- or large-homology). Number in parenthesis indicates number of junctions of each type. Junction profile is not significantly different in *wt* and UNG-deficient mice ($p=0.65$, $p=0.15$ and $p=0.28$ for S_{μ}-$S_{\gamma 1}$, S_{μ}-$S_{\gamma 3}$ and S_{μ}-S_{α} respectively; chi-squared test). Results are pooled from three to five mice per experiments. C: Breakpoint localizations in S_{μ}-$S_{\gamma 1}$, S_{μ}-$S_{\gamma 3}$ and S_{μ}-S_{α} junctions in *wt* and UNG-deficient mice (same junctions as in Figure 1B). D: Motif targeting in S_{μ}-$S_{\gamma 1}$, S_{μ}-$S_{\gamma 3}$ and S_{μ}-S_{α} junctions. Stars identified breakpoint positions in AGCT, WRCY and RGYW AID hotspots and others (same junctions as in Figure 1B).

Figure 1

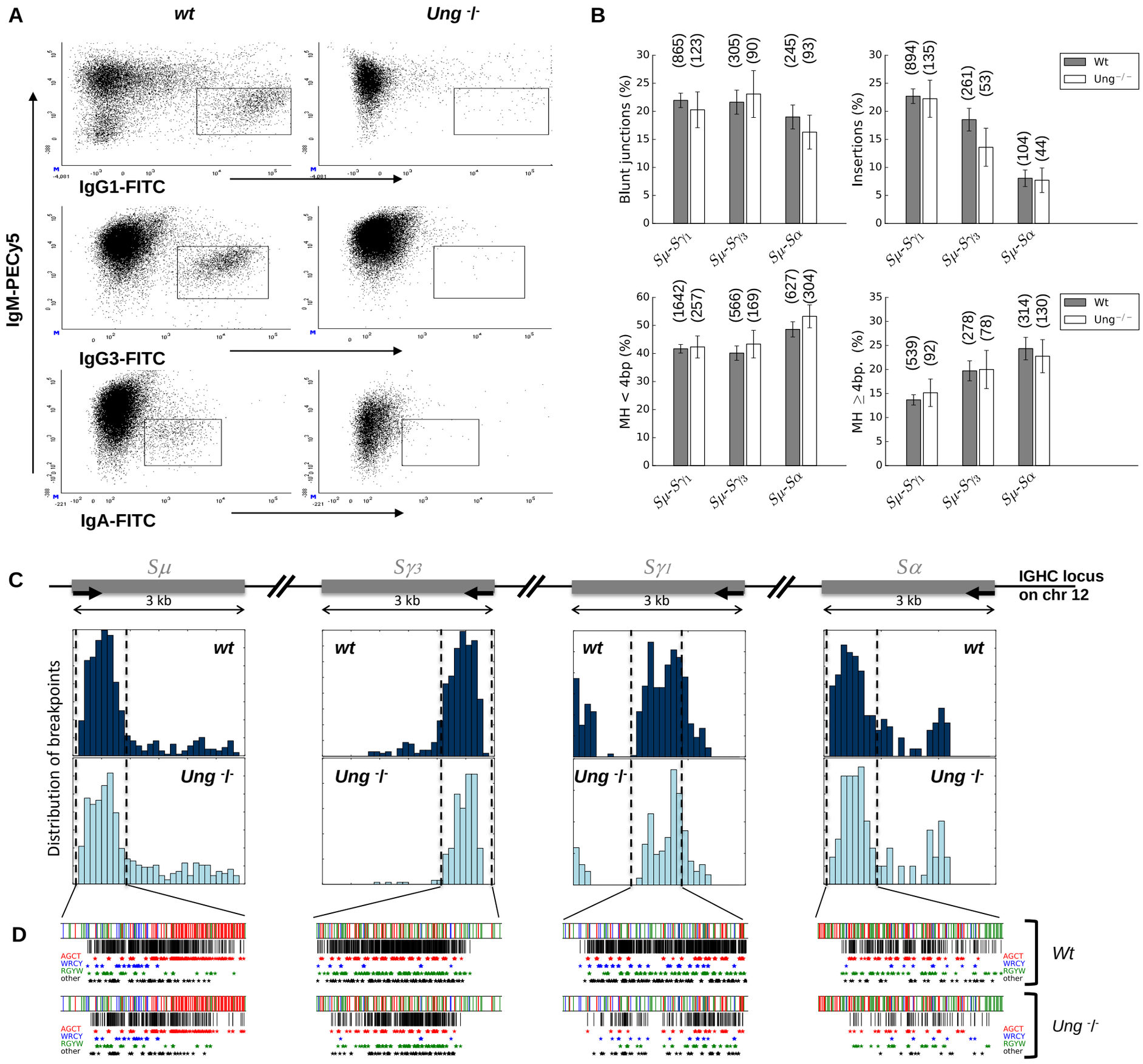
A
wt
Ung -/-
IgM-PECy5
IgG1-FITC
IgG3-FITC
IgA-FITC
B
Blunt junctions (%)
Insertions (%)
MH < 4bp (%)
MH ≥ 4bp. (%)
Wt
Ung−/−
(865) (123)
(305) (90)
(245) (93)
(894) (135)
(261) (53)
(104) (44)
(1642) (257)
(566) (169)
(627) (304)
(539) (92)
(278) (78)
(314) (130)
Sμ-Sγ1
Sμ-Sγ3
Sμ-Sα
C
Sμ
Sγ3
Sγ1
Sα
3 kb
IGHC locus on chr 12
Distribution of breakpoints
wt
Ung -/-
D
AGCT
WRCY
RGYW
other
Wt
Ung -/-